Simple Analytic Approximation for Non-Coherent Radar Detection with Partially Correlated Target RCS and Compound Sea Clutter

Josef A. Zuk
Defence Science and Technology Group, Australia
E-Mail: josef.zuk@dst.defence.gov.au

***Abstract*—We revisit the problem of non-coherent pulse integration in the presence of partially correlated target radar cross-section and clutter, recasting the formulae of Kanter and Weiner to forms that are more transparent and numerically stable. Generalization to compound sea clutter is considered, and an analytic approximation that can cater for a large number of integrated pulses is derived which is simple, explicit and computationally efficient, making it suitable for use in operational simulations of airborne maritime surveillance.**

I. Introduction

Computational radar performance models are important components of constructive and human-in-the-loop (HIL) simulations of airborne maritime surveillance and combat operations [1]. To be fit for purpose, they are required to be computationally efficient while sufficiently accurate, and agile – having the ability to account for the multitude of different conditions encountered during a mission. High-resolution interaction with the sea surface requires the modelling of radar returns exhibiting non-trivial statistics and correlations, typically described by K or Pareto compound sea-clutter models with correlated speckle. In the absence of frequency agility, one must also deal with correlated target radar cross-section (RCS) that is intermediate between the Swerling classes. Moreover, systems that employ scan-to-scan feedback integration will experience correlations induced by the signal processing scheme, which are impervious to frequency agility.

General exact calculations for detection probability resulting from non-coherent pulse integration were given by Kanter [2] for partially correlated Rayleigh fluctuating target RCS, and by Weiner [3] for chi-squared targets. Various simplified special cases had been previously considered. A discussion of Kanter's model in which both the target RCS and clutter returns are present and partially correlated was given in [4]. A review of the subject area is provided in [5]. More recently, efficient approximations to the numerically unstable exact results have been developed, based on saddle-point techniques [6], and effective number-of-looks concepts [7], [8].

We revisit the Kanter and Weiner models, and provide alternative better-behaved exact representations in the presence of multiple correlated signal sources, expressed in terms of Swerling distributions. We also develop a novel light-weight approximation scheme in which the computational load for general correlation is essentially the same as that in the fully correlated Swerling limit.

II. Partial Correlation

We show that the Hubbard-Stratonovich (HS) transformation provides an elegant way to analyse Kanter's model – which considers square-law detection followed by M-pulse non-coherent integration – in the presence of multiple partially correlated signal/noise power sources. The test statistic that determines the detection threshold is the summed returned power random variable (RV)

$$Z = \tfrac{1}{2} \sum_{\eta=\mathrm{i,q}} \Big| \sum_{\alpha} \mathbf{X}_{\eta\alpha} \Big|^2 , \tag{1}$$

where $\mathbf{X}_{\eta\alpha}$ is an M-dimensional vector with elements $X_{\eta\alpha m}$, $m = 1, 2, \ldots, M$. For $\eta = \mathrm{i}, \mathrm{q}$, the $X_{\eta\alpha m}$ are respectively the in-phase and quadrature components on the m-th integrated pulse for power source α. The species index α will typically range over thermal noise (n), target return (s) and various types of clutter (c).

The probability density function (PDF) $P_Z(z)$ of the RV Z is the inverse Laplace transform of the moment generating function (MGF)

$$L_Z(s) \;\equiv\; \big\langle e^{-sZ} \big\rangle_Z \;=\; \left[\Big\langle e^{-\frac{s}{2}\left(\sum_\alpha \mathbf{X}_\alpha\right)^2} \Big\rangle_{\mathbf{X}_\alpha} \right]^2 , \tag{2}$$

where $\mathbf{X}_\alpha$, representing a *single* quadrature component, is distributed identically with $\mathbf{X}_{\mathrm{i}\alpha}$ and $\mathbf{X}_{\mathrm{q}\alpha}$. The entangled species dependence in $L_Z(s)$ may be decoupled with the aid of the HS transformation, the basis of which is the identity

$$e^{-sx^2/2} = \frac{1}{\sqrt{2\pi s}} \int_{-\infty}^{+\infty} du\, e^{-u^2/(2s)} e^{-jux} . \tag{3}$$

When applied to the M-dimensional vector RVs $\mathbf{X}_\alpha$, this yields the relationship

$$\begin{aligned} \Big\langle e^{-\frac{s}{2}\left(\sum_\alpha \mathbf{X}_\alpha\right)^2} \Big\rangle_{\mathbf{X}_\alpha} = \int_{-\infty}^{+\infty} \frac{d^M u}{(2\pi s)^{M/2}}\, e^{-\mathbf{u}\cdot\mathbf{u}/(2s)} \\ \times \prod_\alpha \big\langle e^{-j\mathbf{u}\cdot\mathbf{X}_\alpha} \big\rangle_{\mathbf{X}_\alpha} . \end{aligned} \tag{4}$$

Suppose now that, for each species α, with returned power σ_α^2 and correlation matrix C_α, the joint PDF of the vector RV $\mathbf{X}_\alpha$ is a mean-zero correlated Gaussian:

$$P_{\mathbf{X}_\alpha}(\mathbf{x}) = \frac{1}{(2\pi\sigma_\alpha^2)^{M/2}} \cdot \frac{1}{\sqrt{\det C_\alpha}} \exp\left[-\frac{1}{2\sigma_\alpha^2} \mathbf{x}^{\mathsf{T}} C_\alpha^{-1} \mathbf{x} \right] , \tag{5}$$

where it is assumed that $\mathrm{Tr}\, C_\alpha = M$. It follows directly that

$$\left\langle e^{-j\mathbf{u}\cdot\mathbf{X}_\alpha}\right\rangle_{\mathbf{X}_\alpha} = \exp\left[-\frac{\sigma_\alpha^2}{2}\mathbf{u}^{\mathsf{T}} C_\alpha \mathbf{u}\right] . \tag{6}$$

Therefore,

$$\sqrt{L_Z(s)} = \int_{-\infty}^{+\infty} \frac{d^M u}{(2\pi s)^{M/2}}\, e^{-\mathbf{u}^{\mathsf{T}}\left(s^{-1}\mathbb{I}+\sum_\alpha \sigma_\alpha^2 C_\alpha\right)\mathbf{u}/2} , \tag{7}$$

which is evaluated as

$$L_Z(s) = \left[\det\Big(\mathbb{I} + s\sum_\alpha \sigma_\alpha^2 C_\alpha\Big)\right]^{-1} = \prod_{m=1}^{M} \frac{1}{1+s\lambda_m} , \tag{8}$$

where the λ_m are the eigenvalues of the matrix $\sum_\alpha \sigma_\alpha^2 C_\alpha$, all assumed to be non-degenerate. The associated survival function (*i.e.* complementary cumulative distribution function), obtained via inverse Laplace transform of Eq. (8), may be expressed as

$$\bar{F}_Z(z) = \sum_{m=1}^{M} \Gamma_m e^{-z/\lambda_m} ,\ 1/\Gamma_m \equiv \prod_{\substack{\ell=1\\ \ell\neq m}}^{M} (1-\lambda_\ell/\lambda_m) , \tag{9}$$

Also, the cumulant generating function, given by

$$K(t) \ \equiv\ \ln\left\langle e^{tZ}\right\rangle_Z \ =\ \sum_{n=1}^{\infty} \frac{t^n}{n}\,\mathrm{Tr}\Big(\sum_\alpha \sigma_\alpha^2 C_\alpha\Big)^n , \tag{10}$$

allows us to easily compute the mean and variance of the total returned power Z.

To make contact with the the results of [2] and [3], we shall temporarily restrict our attention to partially correlated target returns in uncorrelated thermal noise. Then, the MGF for target RCS fluctuation class κ ($\kappa = 1, 2, \ldots$), that interpolates between the Swerling $2\kappa-1$ and 2κ limits, can be expressed as

$$\begin{aligned} L_{Z_{\text{avg}}}(s) = {} & \frac{1}{\left(1+\sigma_{\text{n}}^2 s/M\right)^M} \\ & \times \prod_{m=1}^{M}\left[\frac{1+\sigma_{\text{n}}^2 s/M}{1+(\sigma_{\text{n}}^2 s/M)\cdot(1+\gamma_m S/\kappa)}\right]^\kappa , \end{aligned} \tag{11}$$

where $Z_{\text{avg}} \equiv Z/M$ and the γ_m are the eigenvalues of the target correlation matrix C_{s}. For $\kappa = 1$, one can make the identification $\lambda_m = \sigma_{\text{n}}^2\,(1+\gamma_m S)$, with σ_{n}^2 denoting the noise power and $S \equiv \sigma_{\text{s}}^2/\sigma_{\text{n}}^2$ the signal-to-noise ratio (SNR).

The case $\kappa = 1$, which is a direct consequence of Eq. (8), represents Kanter's problem, for which the survival function becomes

$$\bar{F}_{Z'_{\text{avg}}}(z) = \sum_{m=1}^{M} w_m \bar{F}_{\text{avg}}^{\text{SW1}}\left(z;\gamma_m S/M\right) , \tag{12}$$

where here $Z'_{\text{avg}} \equiv Z_{\text{avg}}/\sigma_{\text{n}}^2$, and the weights w_m are given as in Eq. (17). The quantity $\bar{F}_{\text{avg}}^{\text{SW}k}(z;S,M)$ denotes the survival function for the M-pulse Swerling-k problem, normalized such that

$$\int_0^\infty dz\, \bar{F}_{\text{avg}}^{\text{SW}k}(z;S,M) \ =\ \langle Z'_{\text{avg}}\rangle \ =\ 1+S , \tag{13}$$

and we drop the final parameter when its value is clear from the context. With standard double-precision floating-point arithmetic, the largest value of M for which Eq. (12) yields a numerically valid result can be estimated by

$$M_{\max} \approx 13/\log_{10}(1/\rho_{\text{s}}) , \tag{14}$$

with the correlation coefficient ρ_{s} as given in Eq. (22). This represents a considerable improvement on the performance on Kanter's original formula given by Eq. (9).

The case $\kappa = 2$, which requires a slight extension of the derivation leading to Eq. (8) (see Section VI), expresses Weiner's problem, and yields the new representation

$$\begin{aligned} \bar{F}_{Z'_{\text{avg}}}(z) = \sum_{m=1}^{M} w_m^2 \big[& \bar{F}_{\text{avg}}^{\text{SW3}}\left(z;\gamma_m S/M\right) \\ & + 2\zeta_m\, \bar{F}_{\text{avg}}^{\text{SW1}}\left(z;\gamma_m S/(2M)\right)\big] , \end{aligned} \tag{15}$$

with

$$\zeta_m \equiv \sum_{\substack{\ell=1\\ \ell\neq m}}^{M} \frac{\gamma_\ell}{\gamma_\ell - \gamma_m} , \tag{16}$$

which is simpler and considerably more intuitive than the form presented in [3]. One advantage of the Swerling-based formalism is that the weight factors are independent of the SNR S. Furthermore, the Swerling distributions provide a more natural basis than the exponential function for expressing the resulting probabilities, as the vanishing of the correct number of derivatives at the origin is inherent, in contrast to relying on multiple delicate cancelations.

The Swerling-based representations of the survival function apply equally to general aggregated correlation matrices C. Here, the γ_m are the eigenvalues of C, and the weights w_m are computed from them according to

$$\{\gamma_1, \gamma_2, \ldots, \gamma_M\} = \mathrm{eig}(C),\ 1/w_m = \prod_{\substack{\ell=1\\ \ell\neq m}}^{M} (1-\gamma_\ell/\gamma_m) . \tag{17}$$

In particular, in the presence of both a correlated target (C_{s}) and correlated clutter (C_{c}), one may bundle the correlations into a single aggregated correlation matrix according to

$$C_{\text{sig}} \equiv \frac{S}{S+q} C_{\text{s}} + \frac{q}{S+q} C_{\text{c}} , \tag{18}$$

where $0 \le q \le 1$ denotes the clutter-to-interference ratio $q \equiv \sigma_{\text{c}}^2/\sigma_{\text{I}}^2$, with $\sigma_{\text{I}}^2 \equiv \sigma_{\text{n}}^2 + \sigma_{\text{c}}^2$ being the total interference power. Here, $S = \sigma_{\text{s}}^2/\sigma_{\text{I}}^2$ represents the signal-to-interference ratio (SIR). For the $\kappa = 1$ case, with $\{\gamma_1, \gamma_2, \ldots, \gamma_M\} = \mathrm{eig}(C_{\text{sig}})$, this leads to the result

$$\bar{F}_{Z'_{\text{avg}}}(z) = \sum_{m=1}^{M} w_m \bar{F}_{\text{avg}}^{\text{SW1}}\left(\frac{z}{1-q}; \frac{\gamma_m}{M}\cdot\frac{S+q}{1-q}\right) , \tag{19}$$

where now $Z'_{\text{avg}} = Z_{\text{avg}}/\sigma_{\text{I}}^2$.

III. Effective Number of Looks

We shall use the effective-looks concept [8], [9], [10] as a variance matching device in developing a robust approximation to Eq. (19) that overcomes the limitations of Eq. (14).

In order to apply Eq. (10) to Kanter's problem with clutter, we let α span the range $\alpha = \text{n}, \text{c}, \text{s}$ and note that $C_{\text{n}} = \mathbb{I}$ for

thermal noise. Then, we obtain $\langle Z_{\rm avg}/\sigma_{\rm n}^2\rangle = 1 + \mathsf{CNR} + \mathsf{SNR}$, with $\mathsf{SNR} \equiv \sigma_{\rm s}^2/\sigma_{\rm n}^2$, $\mathsf{CNR} \equiv \sigma_{\rm c}^2/\sigma_{\rm n}^2$, and find that the correlation structure can be summarized as

$$\begin{aligned}\mathrm{var}(Z_{\rm avg}/\sigma_{\rm n}^2) = \frac{1}{M} + \frac{\mathsf{CNR}^2}{L} + \frac{\mathsf{SNR}^2}{B} \\ + 2\left(\frac{\mathsf{CNR}}{M} + \frac{\mathsf{SNR}}{M} + \frac{\mathsf{CNR}\cdot\mathsf{SNR}}{N}\right)\,,\end{aligned} \tag{20}$$

where

$$L = M^2/\,\mathrm{Tr}\,C_{\rm c}^2,\ B = M^2/\,\mathrm{Tr}\,C_{\rm s}^2,\ N \equiv M^2/\,\mathrm{Tr}\,C_{\rm c}C_{\rm s}. \tag{21}$$

The quantities L and B are identified with the effective numbers of looks [10] in target and clutter, respectively, while N is a cross-correlation absent in the effective looks formalism.

In a Gauss-Markov correlation model [2], the correlation matrices have the symmetric Toeplitz form:

$$[C_{\rm s}]_{mn} = \rho_{\rm s}^{|m-n|}\,,\quad [C_{\rm c}]_{mn} = \rho_{\rm c}^{|m-n|}\,, \tag{22}$$

where $\rho_{\rm s}$, $\rho_{\rm c}$ are the target and clutter correlation coefficients, respectively, such that $0 \le \rho_{\rm s}, \rho_{\rm c} \le 1$. Then, it is straightforward to confirm that

$$\begin{aligned}B &= M\cdot\left[1 + \frac{2\rho_{\rm s}^2}{1-\rho_{\rm s}^2}\left(1 - \frac{1}{M}\cdot\frac{1-\rho_{\rm s}^{2M}}{1-\rho_{\rm s}^2}\right)\right]^{-1}\,,\\ L &= M\cdot\left[1 + \frac{2\rho_{\rm c}^2}{1-\rho_{\rm c}^2}\left(1 - \frac{1}{M}\cdot\frac{1-\rho_{\rm c}^{2M}}{1-\rho_{\rm c}^2}\right)\right]^{-1}\,,\\ N &= M\cdot\left[1 + \frac{2\rho_{\rm s}\rho_{\rm c}}{1-\rho_{\rm s}\rho_{\rm c}}\left(1 - \frac{1}{M}\cdot\frac{1-(\rho_{\rm s}\rho_{\rm c})^M}{1-\rho_{\rm s}\rho_{\rm c}}\right)\right]^{-1}.\end{aligned} \tag{23}$$

IV. Generalized DMG Model

The model of Dalle Mese and Giuli (DMG) for partially fluctuating targets [11] provides a very simple way to continuously interpolate between Swerling-1 and Swerling-2 statistics, and the result can be expressed entirely in terms of the Swerling-1 PDF. In the DMG model, the RV for the target returns in each pulse is assumed to be a sum of two RVs, independent and identically distributed up to a scale factor. Between pulses, one is assumed to be fast varying — displaying Swerling-2 statistics, while the other is assumed to be slowly varying – displaying Swerling-1 statistics. Thus, suppressing unnecessary indices,

$$X_{\rm s} = X_{\rm s1} + X_{\rm s2}\,, \tag{24}$$

so that the α-index now ranges over the labels $\alpha = {\rm n}, {\rm c}, {\rm s1}, {\rm s2}$, and Kanter's formalism still applies with an additional contribution. Letting

$$\langle X_{\eta{\rm s}}^2\rangle = \sigma_{\rm s}^2\,,\quad \langle X_{\eta{\rm s}1}^2\rangle = \sigma_{\rm s1}^2\,,\quad \langle X_{\eta{\rm s}2}^2\rangle = \sigma_{\rm s2}^2\,, \tag{25}$$

for $\eta = {\rm i}, {\rm q}$, we have $\sigma_{\rm s}^2 = \sigma_{\rm s1}^2 + \sigma_{\rm s2}^2$, and we introduce the correlation coefficient $\rho_{\rm s}$ according to $\rho_{\rm s} \equiv \sigma_{\rm s1}^2/\left(\sigma_{\rm s1}^2 + \sigma_{\rm s2}^2\right)$, so that we can cast the model in terms of the parameters $\sigma_{\rm s}^2$, $\rho_{\rm s}$. Partially correlated clutter can be introduced analogously: $X_{\rm c} = X_{\rm c1} + X_{\rm c2}$. The ensuing survival function may be expressed as

$$\begin{aligned}\bar{F}^{\rm DMG}_{Z'_{\rm avg}}(z;S,q) &= \bar{F}^{\rm SW1}_{\rm avg}\left(\frac{z}{\Lambda(\rho_{\rm c},\rho_{\rm s};S,q)};\frac{\rho_{\rm c}q + \rho_{\rm s}S}{\Lambda(\rho_{\rm c},\rho_{\rm s};S,q)}\right)\,,\\ \Lambda(\rho_{\rm c},\rho_{\rm s};S,q) &\equiv 1 - q + (1-\rho_{\rm c})q + (1-\rho_{\rm s})S\,.\end{aligned} \tag{26}$$

One may note that the covariance matrix that produces the DMG model in Kanter's formalism has the form

$$C_{mn} = \rho + (1-\rho)\delta_{mn}\,, \tag{27}$$

where ρ may refer either to clutter of target RCS. It may be noted that the elements of this matrix do not approach zero as the inter-pulse separation $|m-n|$ increases. Therefore, for any value of the correlation coefficient ρ, the correlated Swerling-1 component will dominate when M is made sufficiently large. For this reason, the original model is rather unphysical.

The variance of the DMG model can be cast into the form

$$\mathrm{var}(Z_{\rm avg}) = \frac{\sigma_{\rm n}^4}{M} + \frac{\sigma_{\rm c}^4}{L} + \frac{\sigma_{\rm s}^4}{B} + 2\left(\frac{\sigma_{\rm n}^2\sigma_{\rm c}^2}{M} + \frac{\sigma_{\rm n}^2\sigma_{\rm s}^2}{M} + \frac{\sigma_{\rm c}^2\sigma_{\rm s}^2}{N}\right)\,, \tag{28}$$

on making the effective-looks identifications

$$\begin{aligned}B &= M/[1 + (M-1)\rho_{\rm s}^2]\,,\\ L &= M/[1 + (M-1)\rho_{\rm c}^2]\,,\\ N &= M/[1 + (M-1)\rho_{\rm c}\rho_{\rm s}]\,,\end{aligned} \tag{29}$$

which imply the relationship

$$N = M/[1 + \sqrt{(M/L-1)(M/B-1)}]\,. \tag{30}$$

Thus, we obtain the same correlation structure as in Kanter's Gauss-Markov model, apart from the difference in the $N(B,L)$ relationship.

The performance of the DMG model, as a proxy for realistic correlations, may be improved by requiring that it reproduce the correct variance. This is achieved by using it with effective correlation coefficients $\rho'_{\rm s}, \rho'_{\rm c}$ that are obtained by solving Eq. (29) in terms of the true effective look numbers B, L, which are, in turn, obtained from the true correlation coefficients via Eq. (23). Explicitly,

$$\begin{aligned}\rho'_{\rm s} &= \sqrt{(M/B-1)/(M-1)}\,,\\ \rho'_{\rm c} &= \sqrt{(M/L-1)/(M-1)}\,.\end{aligned} \tag{31}$$

V. Compound Sea Clutter

Compound models of spiky sea clutter are relevant to high range-resolution detection, in which the clutter power distribution naturally splits into a slowly varying texture that modulates the local mean power, and a fast varying speckle component [7]. In this context, the clutter correlations discussed above relate to the speckle. For the texture, we make the usual assumption that it is fully correlated over all pulses within the beam, and uncorrelated from scan to scan. We let $f_\nu(\tau)$ denote the clutter texture PDF normalized to unit mean, with shape parameter ν that controls the spikiness. For K-distributed clutter, we have

$$f_\nu(\tau)d\tau = \frac{e^{-\nu\tau}}{\Gamma(\nu)}\,(\nu\tau)^{\nu-1}\,\nu\cdot d\tau\,, \tag{32}$$

with $\tau, \nu > 0$. Then, the extension of the DMG model to compound clutter reads

$$\begin{aligned}\bar{F}^{\rm DMG}_{Z'_{\rm avg}}(z;S,q) &= \int_0^\infty d\tau\, f_\nu(\tau)\\ &\times \bar{F}^{\rm SW1}_{\rm avg}\left(\frac{z}{\Lambda_\tau(\rho'_{\rm c},\rho'_{\rm s};S,q)};\frac{\rho'_{\rm c}q\tau + \rho'_{\rm s}S}{\Lambda_\tau(\rho'_{\rm c},\rho'_{\rm s};S,q)}\right)\,,\end{aligned} \tag{33}$$

where

$$\Lambda_\tau(\rho_c', \rho_s'; S, q) \equiv 1 - q + (1 - \rho_c')q\tau + (1 - \rho_s')S \,. \quad (34)$$

The texture integration is easily performed by means of Gaussian quadrature.

The detection probability $P_D(S; q)$ is obtained for a given desired probability of false alarm P_{FA} by solving the equation

$$P_{FA} = P_{FA}(z_b; q) \equiv \bar{F}_{Z'_{avg}}(z_b; 0, q) \,, \quad (35)$$

for the relevant threshold level z_b, and inserting it into the full survival function, so that

$$P_D(S; q) = \bar{F}_{Z'_{avg}}(z_b; S, q) \,. \quad (36)$$

The approximate DMG threshold is obtained by taking the survival function appearing in Eq. (35) to be given by Eq. (33). The exact threshold z_b can be computed from Eq. (19) upon setting the SIR to zero and applying the texture integration. This yields

$$P_{FA}(z_b) = \sum_{m=1}^{M} w_m \int_0^\infty d\tau \, f_\nu(\tau) \bar{F}^{SW1}_{avg}\left(\frac{z_b}{1-q}; \frac{\gamma_m}{M}\frac{q\tau}{1-q}\right)$$
$$\underset{q\to 1^-}{\sim} \sum_{m=1}^{M} w_m \int_0^\infty d\tau \, f_\nu(\tau) e^{-M z_b/(\gamma_m \tau)} \,. \quad (37)$$

For Rayleigh clutter, we take $f_\nu(\tau) = \delta(\tau - 1)$, which is equivalent to the $\nu \to \infty$ limit.

In Figure 1, the false alarm exponent n_{FA} such that $P_{FA} = 10^{-n_{FA}}$ is plotted for the Rayleigh clutter problem against the threshold level z_b, normalized by the mean interference power, in decibels. This has been done for the exact Kanter model (given by Eq. (19)) with Gauss-Markov correlation structure, the DMG approximation to it (given by Eq. (26)), and for the effective looks approach described in [8]. For simplicity, we have assumed that $q = 1$ – corresponding to the clutter-dominated region. The green and magenta curves delineate the full extent of possible variation over all values of the clutter correlation coefficient (being the Swerling 1 and 2 limits). The graphs show that, while the effective-looks and DMG approximations are good in the body of the distribution (*i.e.* around the median), they diverge increasingly from the true value the further one goes into the tail. This suggests that a different approximation scheme that improves in accuracy the further one traverses the tail region, such as a saddle-point approximation [6], should be used for threshold estimation [12].

In Figure 2, the threshold curves from Figure 1 are applied to their respective survival functions (according to Eq. (36)) to yield the detection probability curves for a false-alarm exponent of $n_{FA} = 6$. The dashed curves correspond to the effective-looks and DMG survival functions evaluated at the exact threshold level, rather than those derived within their respective approximation schemes. We see that excellent fits are obtained in both cases provided that exact thresholds are used. The discrepancies in the solid curves between exact and approximate results arise from the poor threshold estimation observed in Figure 1.

Figure 3 shows the same quantities as Figure 1, but for K-distributed compound clutter with shape parameter $\nu = 5$.

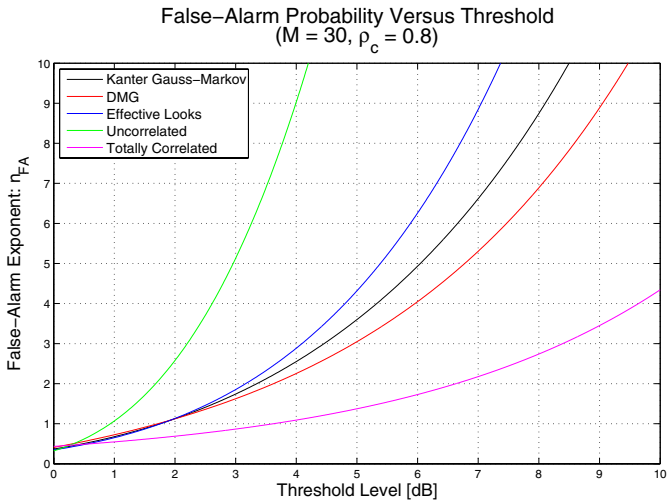

Fig. 1. False-alarm exponent versus threshold level for $M = 30$ pulses and clutter correlation coefficient $\rho_c = 0.8$.

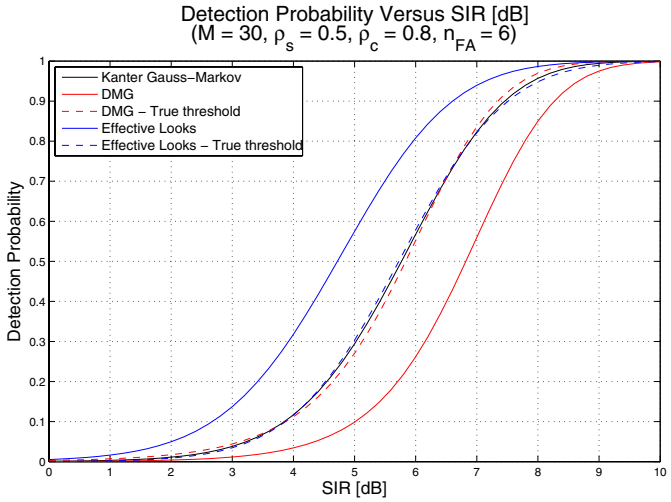

Fig. 2. Detection probability for $M = 30$ pulses, clutter correlation coefficient $\rho_c = 0.8$, target RCS correlation coefficient $\rho_s = 0.5$, and false-alarm exponent $n_{FA} = 6$. The effective looks in this case are $L = 7.1$, $B = 18.3$.

The results are qualitatively similar, but with considerably less discrepancy in the far tail. This behaviour is expected, as the contribution to the threshold from the body of the speckle distribution, induced by the texture integration, increases with increasing clutter spikiness (*i.e.* decreasing shape parameter). Detection curves incorporating K-distributed clutter with shape parameter $\nu = 5$ are presented in Figure 4. Again, the DMG and effective-looks approaches with true threshold provide very good fits; but the former has the advantage that it does not require the multiple integrations or the extensive series summation associated with the latter.

VI. Higher-Order Correlation

The DMG model is easily generalized to target RCS in fluctuation class $\kappa > 1$. Let us assume uncorrelated Rayleigh clutter, and carry out the noise and clutter expectations in Eq. (4) whilst leaving the target sector intact. The analogue

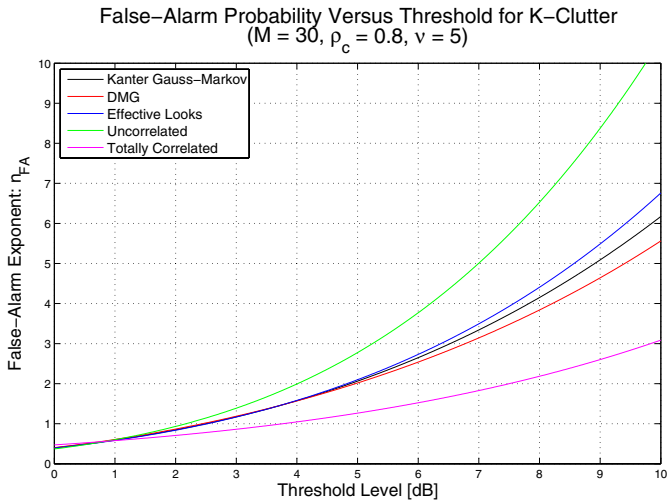

Fig. 3. False-alarm exponent versus threshold level for $M = 30$ pulses and clutter correlation coefficient $\rho_{\rm c} = 0.8$. K-distributed clutter is present with shape parameter $\nu = 5$.

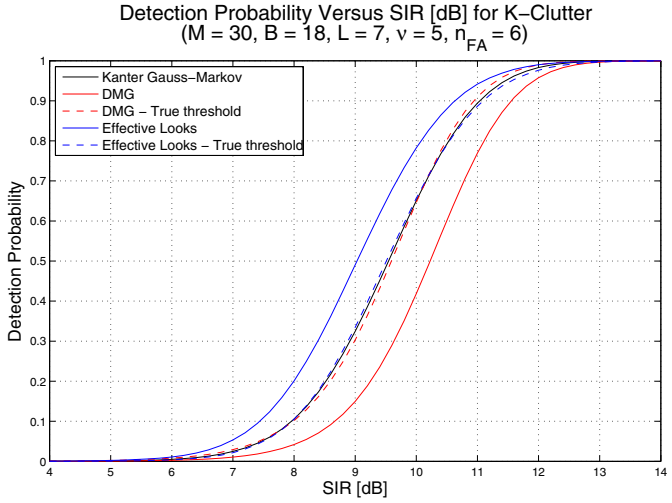

Fig. 4. Detection probability in K-clutter for $M = 30$ pulses, effective clutter looks $L = 18$, effective target looks $B = 7$, and false-alarm exponent $n_{\rm FA} = 6$. The correlation coefficients in this case are $\rho_{\rm s} = 0.51$, $\rho_{\rm c} = 0.80$.

of Eq. (7) is then

$$\begin{aligned}\sqrt{L_Z(s)} &= \int_{-\infty}^{+\infty} \frac{d^M u}{(2\pi s)^{M/2}}\, e^{-\xi^2 \mathbf{u}^2/2} \left\langle e^{-j\mathbf{u}\cdot\mathbf{X}} \right\rangle_{\mathbf{X}} \\ &= \frac{1}{(s\xi^2)^{M/2}} \left\langle e^{-\mathbf{X}^2/(2\xi^2)} \right\rangle_{\mathbf{X}} ,\end{aligned} \tag{38}$$

where $\xi^2 \equiv s^{-1} + \sigma_{\rm I}^2$ and $\mathbf{X}$ represents the vector RV for the (in-phase) target returns. Due to orthogonal invariance of the foregoing integral, the components X_m can, without loss of generality, be considered independent. Thus, given that the RVs X_m^2 are independently distributed according to a gamma distribution with common shape parameter $\kappa/2$ and with respective means $\gamma_m^{\rm s}\sigma_{\rm s}^2$, it follows that [3]

$$\left\langle e^{-X_m^2/(2\xi^2)} \right\rangle_{X_m} = \left(1 + \frac{\gamma_m^{\rm s}\sigma_{\rm s}^2}{\kappa\xi^2}\right)^{-\kappa/2} . \tag{39}$$

Upon combining these results, we reproduce Eq. (11) with the noise power $\sigma_{\rm n}^2$ replaced by the interference power $\sigma_{\rm I}^2$, and S interpreted as the SIR. In the DMG model,

$$\gamma_m^{\rm s} = \begin{cases} 1-\rho_{\rm s}' & \text{for} \quad m = 1, 2, \ldots, M-1\,, \\ 1-\rho_{\rm s}' + M\rho_{\rm s}' & \text{for} \quad m = M\,. \end{cases} \tag{40}$$

Hence, Eq. (11) reduces to

$$L_{Z_{\rm avg}}(s) = \left[\frac{1+as'}{1+(a+b)s'}\right]^{\kappa} \left[\frac{(1+s')^{\kappa-1}}{(1+as')^{\kappa}}\right]^{M} , \tag{41}$$

where we have set

$$s' \equiv s\sigma_{\rm I}^2/M, a \equiv 1 + (1-\rho_{\rm s}')S/\kappa,\ b \equiv M\rho_{\rm s}'S/\kappa\,. \tag{42}$$

This MGF interpolates in a very simple manner between $L_{{\rm SW}(2\kappa)}(s)$ for $\rho_{\rm s}' = 0$ and $L_{{\rm SW}(2\kappa-1)}(s)$ for $\rho_{\rm s}' = 1$, and leads to the survival function

$$\begin{aligned}\bar{F}_{Z_{\rm avg}'}^{{\rm DMG}\kappa}(z) = &\sum_{k=0}^{(\kappa-1)M} \binom{(\kappa-1)M}{k} \left(\frac{1}{a}\right)^{M-k} \left(1-\frac{1}{a}\right)^{k} \\ &\times \bar{F}_{\rm avg}^{{\rm SW}(2\kappa-1)}\left(\frac{Mz}{a(M+k)}; \frac{\kappa b/a}{M+k}, M+k\right) .\end{aligned} \tag{43}$$

Inclusion of correlated Rayleigh clutter $\rho_{\rm c}' > 0$ from first principles is problematic because the orthogonal symmetry observed in Eq. (38) no longer holds. The specification of the higher-order Swerling models in terms of only power distributions [13] is not sufficient here. It is necessary to account also for the phase between the underlying quadrature RVs. A similar issue for clutter is discussed in [14], where it is pointed out that the random phase between quadrature components is correlated even in the Gaussian problem unless it comprises entirely white noise (*i.e.* $\rho = 0$). We are presently unaware of any complete model having been proposed that possesses all the obviously desirable properties. Nevertheless, we postulate as the DMG approximation to the general problem ($\rho_{\rm s}', \rho_{\rm c}' > 0$, $\kappa \geq 1$) the MGF

$$L_{Z_{\rm avg}}(s) = \frac{[1+(1+c)s']^{\kappa-1}}{[1+(a+b)s']^{\kappa}} \left[\frac{(1+s')^{\kappa-1}}{(1+as')^{\kappa}}\right]^{M-1} , \tag{44}$$

where now $s' \equiv s\sigma_{\rm nc}^2/M$, and

$$a \equiv \sigma_{\rm ns}^2/\sigma_{\rm nc}^2\,,\ b \equiv \sigma_{\rm ss}^2/(\kappa\sigma_{\rm nc}^2)\,,\ c \equiv \sigma_{\rm sc}^2/(\kappa\sigma_{\rm nc}^2)\,, \tag{45}$$

with

$$\sigma_{\rm nc}^2 \equiv \sigma_{\rm n}^2 + (1-\rho_{\rm c}')\sigma_{\rm c}^2\,,\ \sigma_{\rm ns}^2 \equiv \sigma_{\rm nc}^2 + (1-\rho_{\rm s}')\sigma_{\rm s}^2/\kappa\,. \tag{46}$$

and

$$\sigma_{\rm sc}^2 \equiv \kappa M\rho_{\rm c}'\sigma_{\rm c}^2\,,\ \sigma_{\rm ss}^2 \equiv \sigma_{\rm sc}^2 + M\rho_{\rm s}'\sigma_{\rm s}^2\,. \tag{47}$$

This form is motivated by fact that it has been constructed to faithfully reproduce the DMG approximations for a number of special cases, including (i) $\rho_{\rm c}' = 0$ for all $\kappa, \rho_{\rm s}'$, (ii) $\rho_{\rm s}' = 0$ for all $\kappa, \rho_{\rm c}'$, (iii) $\kappa = 1$ for all $\rho_{\rm s}', \rho_{\rm s}'$. We have tested the model for $\kappa = 2$, whose survival function comprises that of Eq. (43) with updated parameters according to Eq. (45) (which necessitates the mapping $z \mapsto z/(1-\rho_{\rm c}'q)$ on the RHS of Eq. (43)) plus a correction term that vanishes for $\rho_{\rm c}' = 0$. The results match closely those predicted for the same correlation structure by the

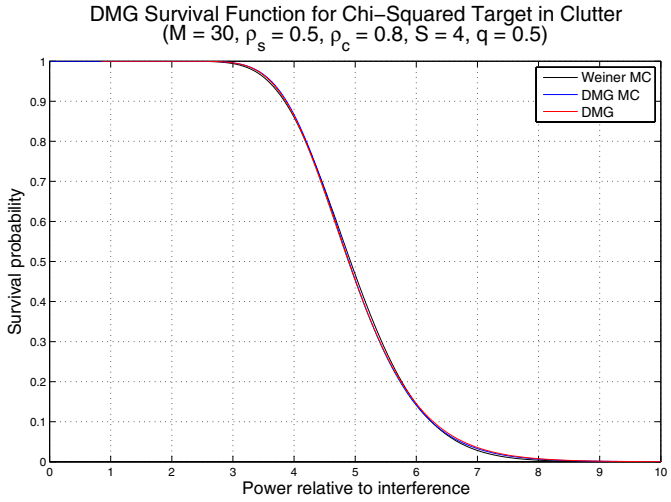

Fig. 5. Survival function for $M = 30$ pulses and clutter correlation coefficient $\rho_{\rm c} = 0.8$, target correlation coefficient $\rho_{\rm s} = 0.5$, with $S = 4$, $q = 0.5$.

effective-looks approach described in [8] for all cases tested. Explicitly, the aforementioned correction term reads

$$\Delta\bar{F}^{\rm DMG2}_{Z'_{\rm avg}}(z) = \frac{c}{a+b}\sum_{k=0}^{M-1}\binom{M-1}{k}\left(\frac{1}{a}\right)^{M-1-k}\left(1-\frac{1}{a}\right)^{k} \times\left[\bar{F}^{\rm SW1}_{\rm avg}\left(\frac{Mz/(1-\rho'_{\rm c}q)}{a(M+k)};\frac{b/a}{M+k},M+k\right)\right. \left.-\,\bar{F}^{\rm SW3}_{\rm avg}\left(\frac{Mz/(1-\rho'_{\rm c}q)}{a(M+k+1)};\frac{2b/a}{M+k+1},M+k+1\right)\right]. \quad (48)$$

A sanity check is provided by considering the special case $S = 0$.

Comparison with an established exact result is not possible, as discussed above. However, we have developed two candidate phase processes for the target quadrature components that reduce correctly to the Gaussian case ($\kappa = 1$) and satisfy almost all other expectations. The survival functions for the exact theory incorporating these processes, obtained by Monte Carlo (MC) simulation, lie close to the DMG curve, and bound it from above and below. These results will be further developed and presented in future work.

In Figure 5, we present a sample survival function for a partially correlated chi-squared target ($\kappa_{\rm s} = 2$) in partially correlated Rayleigh clutter ($\kappa_{\rm c} = 1$) within the generalized DMG model of Eq. (44). It is compared with a MC simulation of the same model (which serves as a check of the algebra leading to Eq. (48)), and with a first-principles MC simulation of the exact Weiner-type theory, assuming one of the phase processes discussed above. Good agreement is observed here and for all other cases tested.

For the higher-order DMG model with compound sea clutter, the texture integration is incorporated analogously to that of the basic model in Eq. (33), via the mapping $\sigma_{\rm c}^2 \mapsto \sigma_{\rm c}^2\tau$ in Eqs. (46) and (47).

VII. Conclusions

We have derived alternative, better behaved, exact representations for the detection probability models of Kanter and Weiner associated with non-coherent integration in the presence of partially correlated target RCS, and the scope of Kanter's model has been extended to include partially correlated compound sea clutter. We have also derived a simple analytic approximation that can deal with a large number of integrated pulses, and accounts for speckle-correlated compound clutter distributions.

The resulting generalized DMG model exhibits an accuracy comparable with that of the effective-looks approach [8], [12] but is very much simpler to compute, making it suitable for incorporation into constructive and HIL simulation of maritime radar surveillance operations.

All results derived here have been verified using MC simulation with RVs and their correlations generated at the lowest possible (*i.e.* quadrature component) level, and have also tested with a Gauss-Toeplitz correlation structure, such that $C_{mn} = \rho^{(m-n)^2}$. Compound sea clutter calculations have been replicated with the Pareto model.

References

[1] P. Sheehan and J. Mukerjee, "Application of desktop human in the loop simulation to study air operations," in *21st International Congress on Modelling and Simulation*, Gold Coast, Australia, Nov. 2015. [Online]. Available: http://www.mssanz.org.au/modsim2015

[2] I. Kanter, "Exact detection probability for partially correlated Rayleigh targets," *IEEE Transactions on Aerospace and Electronic Systems*, vol. 22, no. 2, pp. 184–196, Mar. 1986.

[3] M. Weiner, "Detection probability for partially correlated chi-square targets," *IEEE Transactions on Aerospace and Electronic Systems*, vol. 24, no. 4, pp. 411–416, Jul. 1988.

[4] X.-Y. Hou and N. Morinaga, "Detection performance of Rayleigh fluctuating targets in correlated Gaussian clutter plus noise," *The Transactions of the Institute of Electronics, Information and Communication Engineers (IEICE)*, vol. E.71, no. 3, pp. 208–217, Mar. 1988.

[5] A. Buterbaugh, "The detection and correlation modeling of Rayleigh distributed radar signals," Air Force Institute of Technology, Master's Thesis AFIT/GE/ENG/92S-03, Sep. 1992.

[6] C. Helstrom, "Detection probabilities for correlated Rayleigh fading signals," *IEEE Transactions on Aerospace and Electronic Systems*, vol. 28, no. 1, pp. 259–267, Jan. 1992.

[7] K. Ward, R. Tough, and S. Watts, *Sea Clutter: Scattering, the K-Distribution and Radar Performance*, 2nd ed. London, UK: The Institute of Engineering Technology, 2013.

[8] L. Rosenberg and S. Bocquet, "Non-coherent radar detection performance in medium grazing angle X-band sea clutter," *IEEE Transactions on Aerospace and Electronic Systems*, vol. 52, no. 2, pp. 669–682, Apr. 2017.

[9] D. Barton, "Simple procedures for radar detection calculations," *IEEE Transactions on Aerospace and Electronic Systems*, vol. 5, no. 5, pp. 837–846, Sep. 1969.

[10] F. Nathanson, *Radar Design Principles*, 2nd ed. Mendham, NJ: Scitech Publishing, 1999.

[11] E. Dalle Mese and D. Giuli, "Detection probability of a partially fluctuating target," *IEE Proceedings, Part F*, vol. 131, no. 1, pp. 179–182, Apr. 1984.

[12] S. Bocquet, J. Zuk, and L. Rosenberg, "Non-coherent radar detection probability in compound sea clutter with correlated speckle," To be presented at the 2018 IEEE Radar Conference, Oklahoma City, OK, USA, Apr. 2018.

[13] P. Swerling, "Detection of fluctuating pulsed signals in the presence of noise," *IRE Transactions on Information Theory*, vol. 3, no. 3, pp. 175–178, Sep. 1957.

[14] E. Conte and M. Longo, "Characterization of radar clutter as a spherically invariant random process," *IEE Proceedings, Part F*, vol. 134, no. 2, pp. 191–197, Apr. 1987.